SFB/CPP-06-09
TTP06-09

Complete Higgs mass dependence of top quark pair threshold production to order $\alpha\alpha_s$

D. Eiras and M. Steinhauser

Institut für Theoretische Teilchenphysik, Universität Karlsruhe

76128 Karlsruhe, Germany

Abstract

In this paper we consider the production of top quark pairs close to threshold and compute the dependence on the Higgs boson mass to order $\alpha\alpha_s$. This requires the evaluation of the matching coefficient of the vector current to two-loop level and the inclusion of Higgs mass dependent operators in the non-relativistic effective theory. For Higgs boson masses below 200 GeV moderate contributions to the top quark mass and the peak cross section are observed. We also provide additional information to the on-shell wave function renormalization which is relevant for the matching coefficient.

PACS numbers: 14.65.Ha, 14.80.Bn

1 Introduction

One of the most important tasks of a future international linear collider (ILC) [1] is the precise measurement of the cross section for the production of top quark pairs close to threshold. The comparison with theoretical calculations will lead to a determination of the top quark mass with an unrivaled precision leading to an uncertainty below 100 MeV [2]. Furthermore, also the width of the top quark, the strong coupling and the Yukawa coupling between the top quark and Higgs boson can be extracted from such a measurement. The findings of this paper are important in this context. However, the final success of such an enterprise depends crucially on whether the theoretical precision can match the expected experimental one. The complete next-to-next-to-leading analysis of Ref. [3] has shown that it is important to obtain the third-order result within QCD. This constitutes a long-term calculation which has already been started (see, e.g., Refs. [4, 5] for the most recent results).

The naive scaling rule $\alpha \sim \alpha_s^2$, where α is the fine structure and α_s is the strong coupling constant, shows that the next-to-next-to-next-to-leading terms are parametrically of the same order as the mixed corrections proportional to $\alpha\alpha_s$. In this paper we take the first step to a complete order $\alpha\alpha_s$ result and compute the full dependence on the Higgs boson mass. On one hand this requires the evaluation of two-loop vertex corrections within the Standard Model (SM) involving a Higgs boson and a gluon. Furthermore, a new operator depending on the Higgs mass has to be considered on the effective theory side. As we will explicitly see, the two individual pieces are divergent, however, the physical quantities formed by the proper combination is finite.

Effects from the Higgs boson mass have already been studied in Ref. [6] where a Yukawa-type potential has been used and the Schrödinger equation has been solved numerically in order to obtain the imaginary part of the Green function and finally the total cross section. In this paper we will consider the Higgs boson mass to be much larger than the soft scales involved in the process and include it in a systematic way in the non-relativistic effective theory. The importance of a systematic and careful treatment of electroweak corrections to the top quark pair production has been stressed in Ref. [7, 8], where certain next-to-next-to-leading logarithmic electroweak effects associated to the instability of the top quark have been considered.

The paper is organized as follows: In the next Section we consider the new Higgs mass dependent operator included into non-relativistic QCD (NRQCD) and evaluate the corrections to the energy level and the wave function at the origin. In Section 3 the Higgs mass dependent corrections to the matching coefficient are discussed and Section 4 contains a brief account of the phenomenological applications of our results. We conclude in Section 5. In Appendix A we discuss the results for the matching coefficients induced by vertex corrections involving a Z boson and Appendix B contains additional information on the wave function renormalization constant which is relevant in connection to the matching coefficient.

2 Effective theory

The standard theoretical framework for the threshold production of top quark pairs is given by NRQCD [9, 10] which ensures the automatic resummation of terms like $(\alpha_s/v)^n$ $(n = 1, 2, 3, \ldots)$ where v is the velocity of the produced quarks. NRQCD is constructed from QCD by integrating out the hard scales associated to the mass of the heavy quark, m. Thus it contains only degrees of freedom of the order mv and mv^2.

In this paper we consider next to the top quark, which takes over the role of the heavy quark, also the Higgs boson with mass M_h. Since $M_h \gg m_t v$ both mass scales are integrated out simultaneously. In Ref. [11] all operators which appear within QCD up to third order in perturbation theory have been classified. The only operator which has to be added to the Hamiltonian in Eq. (6) of Ref. [11] is given by

$$\delta\mathcal{H}_H \quad = \quad -\frac{\alpha\pi m_t^2}{s_W^2 M_W^2 M_H^2}\,, \tag{1}$$

where s_W is the sine of the Weinberg angle and M_W is the W boson mass. The corresponding expression in coordinate space is proportional to the delta function. If we employ the counting rule $\alpha \sim \alpha_s^2$ it is easy to see that $\delta\mathcal{H}_H$ gives contributions which are parametrically of the same order as the ones from the third-order QCD Hamiltonian.

Let us in a first step evaluate the corrections to the energy levels induced by the operator $\delta\mathcal{H}_H$. Using first order perturbation theory we obtain

$$\delta E_n^H \quad = \quad \langle\psi_n^C|\delta\mathcal{H}_H|\psi_n^C\rangle \quad = \quad E_n^C \frac{\alpha\alpha_s C_F m_t^4}{2 s_W^2 n M_W^2 M_h^2}\,, \tag{2}$$

with $E_n^C = -C_F^2\alpha_s^2 m_t/(4n^2)$ and ψ_n^C is the Coulomb wave function. n is the principal quantum number.

In order to compute the correction to the wave function at the origin the operator of Eq. (1) has to be inserted into the standard formulae of non-relativistic perturbation theory

$$\delta\psi_n(0) = -\int \mathrm{d}^3\vec{r}\, G_C(0,\vec{r},E)\,\delta\mathcal{H}_H\,\psi_n^C(\vec{r})\,, \tag{3}$$

where G_C is the Coulomb Green function. Following Ref. [12] we split G_C into a contribution with zero, one and infinitely many gluon exchanges. Since only the one-gluon-exchange part is divergent it is convenient to perform the corresponding calculation in momentum space whereas the other contributions are evaluated in coordinate space. As a final result we obtain

$$\delta\psi_n^H(0) \quad = \quad \psi_n^C(0)\frac{\alpha\alpha_s m_t^4}{s_W^2 M_W^2 M_h^2} C_F\left[-\frac{1}{4}\ln\left(\frac{\alpha_s C_F m_t}{\mu}\right) + \frac{3}{8}\right]\,, \tag{4}$$

with $\left|\psi_n^C(0)\right|^2 = C_F^3\alpha_s^3 m_t^3/(8\pi n^3)$. The divergence in Eq. (4) has been subtracted minimally which will also be done for the coefficient function considered in the next section.

We want to mention that the formulae of this Section are adapted for the top quark. However, they also apply to other quark masses, in particular to the bottom system, by simply exchanging the top quark mass.

3 Higgs mass dependence of the matching coefficient

The matching coefficient of the vector current $j^\mu = \bar{t}\gamma^\mu t$ is defined by

$$j_v^k = c_v \phi^\dagger \sigma^i \chi + \mathcal{O}\left(\frac{1}{m_t^2}\right) , \tag{5}$$

where ϕ and χ are two-component Pauli spinors for quark and anti-quark, respectively, and $k = 1, 2, 3$ denote the spacial components. Note that there is no contribution to our order from the time-component.

For the practical computation of c_v it is convenient to consider the $t\bar{t}\gamma$ vertex in the limit where for the photon energy, s, we have $s \approx 4m_t^2$. In this case we can establish the equation

$$Z_2 \Gamma_v \;\; = \;\; c_v \tilde{Z}_2 \tilde{Z}_v^{-1} \tilde{\Gamma}_v + \ldots , \tag{6}$$

where we have on the left- and right-hand side quantities of the full and effective theory, respectively. The latter are marked by a tilde and the ellipses denote terms suppressed by inverse powers of the top quark mass. Γ_v denotes the $t\bar{t}\gamma$ vertex corrections where it is understood that the couplings and masses are renormalized. The two-loop mixed correction to the on-shell wave function renormalization, Z_2, has been computed recently in Ref. [13]. In particular, for the Higgs boson contributions both the exact result and the expansions in three kinematic regions have been provided.

At this point it is convenient to apply the so-called threshold expansion [14, 15] to Eq. (6) which has the consequence that Γ_v has to be evaluated for $s = 4m_t^2$ since all except the hard region cancel in Eq. (6). Furthermore, on the right-hand side only tree contributions have to be considered. In particular we have $\tilde{Z}_2 = 1$.

The one-loop corrections to c_v are finite [16]. However, starting from two-loop order, the matching coefficient exhibits infra-red divergences which are compensated by ultra-violet divergences of the effective theory rendering physical quantities finite. In Eq. (6) the renormalization constant $\tilde{Z}_v$ which generates the anomalous dimension of $\tilde{j}_v$ takes over this part. Note that the vector current in the full theory does not get renormalized.

It is convenient to introduce the perturbative decomposition of the matching coefficient

$$c_v \;\; = \;\; 1 + \frac{\alpha_s}{\pi} C_F c_v^{\mathrm{QCD},1} + \left(\frac{\alpha_s}{\pi}\right)^2 C_F c_v^{\mathrm{QCD},2} + \frac{\alpha}{\pi s_W^2} c_v^{\mathrm{ew}} + \frac{\alpha \alpha_s}{\pi^2 s_W^2} C_F c_v^{\mathrm{mix}} , \tag{7}$$

where analog formulae also hold for Z_2 and Γ_v. Since we consider in this paper only the contribution from the Higgs boson the corresponding quantities obtain an additional superscript H.

The two-loop QCD corrections, $c_v^{\mathrm{QCD},2}$, have been computed in Refs. [17, 18] (see also Ref. [19]). The complete SM corrections to one-loop order can be found in Ref. [16] where next to the vertex corrections also the box diagrams contributing to $e^+e^- \to t\bar{t}$ have been considered. The latter, however, get no contributions from the Higgs boson.

From the perturbative expansion of Eq. (6) it is easy to see that the one-loop results $c_v^{\mathrm{QCD},1}$ and c_v^{ew} are simply given by the sum of the one-loop expressions for Z_2 and Γ_v.

Whereas the individual pieces are still divergent the proper sum is finite. For convenience we repeat the QCD corrections and the Higgs mass dependent term of $c_v^{\rm ew}$ which are given by

$$
\begin{aligned}
c_v^{\rm QCD,1} &= -2\,,\\
c_v^{H,\rm ew} &= \frac{m_t^2}{M_W^2}\left[\frac{3y_H^2-1}{12y_H^2} - \frac{2-9y_H^2+12y_H^4}{48y_H^4}\ln y_H^2 - \frac{(-2+5y_H^2-6y_H^4)}{24y_H^2}\Psi(y_H)\right], \qquad (8)
\end{aligned}
$$

where

$$
\Psi(x) = \begin{cases} \frac{\sqrt{4x^2-1}}{x^2}\arctan\sqrt{4x^2-1} & \text{for } x \geq \frac{1}{2} \\ \frac{\sqrt{1-4x^2}}{2x^2}\ln\frac{1-\sqrt{1-4x^2}}{1+\sqrt{1-4x^2}} & \text{for } x < \frac{1}{2}\,, \end{cases} \qquad (9)
$$

and $y_H = m_t/M_h$.

At two-loop order it is quite difficult to obtain a closed analytic result valid for all Higgs and top quark masses. However, it is possible to get compact formulae valid in various kinematical regions which — when combined — cover the whole Higgs mass range. This strategy has been successfully applied in Ref. [13] to the on-shell wave function renormalization (see also Appendix B). Thus, let us consider $c_v^{H,\rm ew}$ in the limits $m_t \ll M_H$, $m_t \approx M_H$ and $m_t \gg M_H$ where it is given by

$$
\begin{aligned}
c_{v,0}^{H,\rm ew} &= \frac{m_t^2}{M_W^2}\Bigg[y_H^2\left(\frac{31}{144}-\frac{5}{24}\ln y_H^2\right) + y_H^4\left(-\frac{3}{16}-\frac{\ln y_H^2}{4}\right) + y_H^6\left(-\frac{307}{480}-\frac{5\ln y_H^2}{8}\right)\\
&\quad + y_H^8\left(-\frac{737}{360}-\frac{11\ln y_H^2}{6}\right)+\ldots\Bigg],\\
c_{v,1a}^{H,\rm ew} &= \frac{m_t^2}{M_W^2}\Bigg[\frac{1}{6}+\frac{\pi}{8\sqrt{3}} + y_{H,1a}\left(\frac{1}{24}+\frac{\pi}{8\sqrt{3}}\right) + y_{H,1a}^2\left(-\frac{1}{12}+\frac{\pi}{6\sqrt{3}}\right)\\
&\quad + y_{H,1a}^3\left(-\frac{1}{36}+\frac{13\pi}{108\sqrt{3}}\right) + y_{H,1a}^4\left(\frac{1}{288}+\frac{5\pi}{54\sqrt{3}}\right)+\ldots\Bigg],\\
c_{v,1b}^{H,\rm ew} &= \frac{m_t^2}{M_W^2}\Bigg[\frac{1}{6}+\frac{\pi}{8\sqrt{3}} - y_{H,1b}\left(\frac{1}{24}+\frac{\pi}{8\sqrt{3}}\right) + y_{H,1b}^2\left(-\frac{1}{8}+\frac{\pi}{24\sqrt{3}}\right)\\
&\quad - y_{H,1b}^3\left(\frac{13}{72}-\frac{19\pi}{216\sqrt{3}}\right) + y_{H,1b}^4\left(-\frac{59}{288}+\frac{23\pi}{216\sqrt{3}}\right)+\ldots\Bigg],\\
c_{v,\infty}^{H,\rm ew} &= \frac{m_t^2}{M_W^2}\Bigg[\frac{\pi}{4}y_H - \frac{\ln y_H}{2} - \frac{23\pi}{96}\frac{1}{y_H} + \left(\frac{7}{48}+\frac{3}{8}\ln y_H\right)\frac{1}{y_H^2} + \frac{55\pi}{512}\frac{1}{y_H^3}\\
&\quad + \left(-\frac{71}{720}-\frac{\ln y_H}{12}\right)\frac{1}{y_H^4}+\ldots\Bigg], \qquad (10)
\end{aligned}
$$

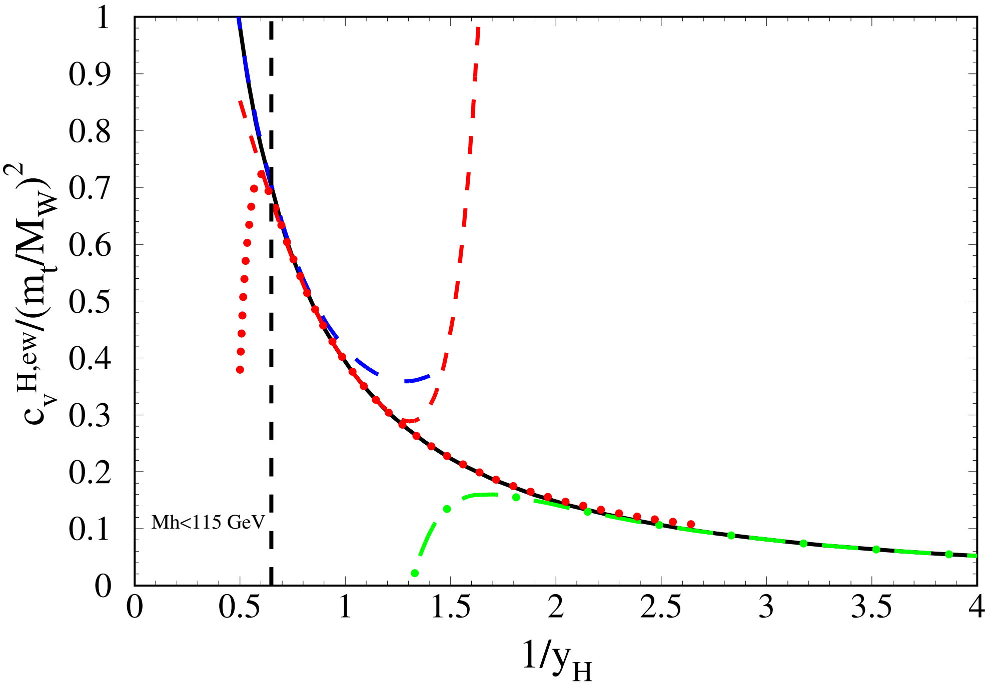

Figure 1: $c_v^{H,\text{ew}}/(m_t^2/M_W^2)$ as a function of $1/y_H$. The solid (black) line represents the exact result. The approximations in the three regions are shown as dotted, dashed and dash-dotted lines where for the expansion around $y_H \approx 1$ two different approximations have been chosen.

with $y_{H,1a} = (1 - 1/y_H^2)$ and $y_{H,1b} = (1 - y_H^2)$. $c_{v,1a}^{H,\text{ew}}$ and $c_{v,1b}^{H,\text{ew}}$ are two different representations of the same information which turn out to be useful for different values of y_H.

In Fig. 1 the exact result for $c_v^{\text{ew}}/(m_t^2/M_W^2)$ (full black line, cf. Eq. (8)) is shown together with the expansions from Eq. (10), $c_{v,0}^{H,\text{ew}}$ (dash-dotted), $c_{v,1a}^{H,\text{ew}}$ (short dashed), $c_{v,1b}^{H,\text{ew}}$ (dotted) and $c_{v,\infty}^{H,\text{ew}}$ (long dashed). One can see that the approximations nicely cover the whole region of y_H. Note that the expansion around $m_t = M_H$ shows better convergence properties in case $y_{H,1b}$ is used as parameter.

Let us draw the attention of the reader to the expansion terms for large top quark masses which starts with an enhancement factor $m_t^3/(M_W^2 M_h)$. Two out of the three powers in m_t come from the Yukawa coupling between the Higgs boson and the top quark and the factor m_t/M_h is the indication of the Coulomb singularity which would be present for a massless Higgs boson. The next-to-leading term is quadratic in m_t accompanied by a logarithm in m_t/M_h. Both terms indicate that even for the leading terms it is not possible to nullify the Higgs boson mass and non-trivial integration regions have to be considered

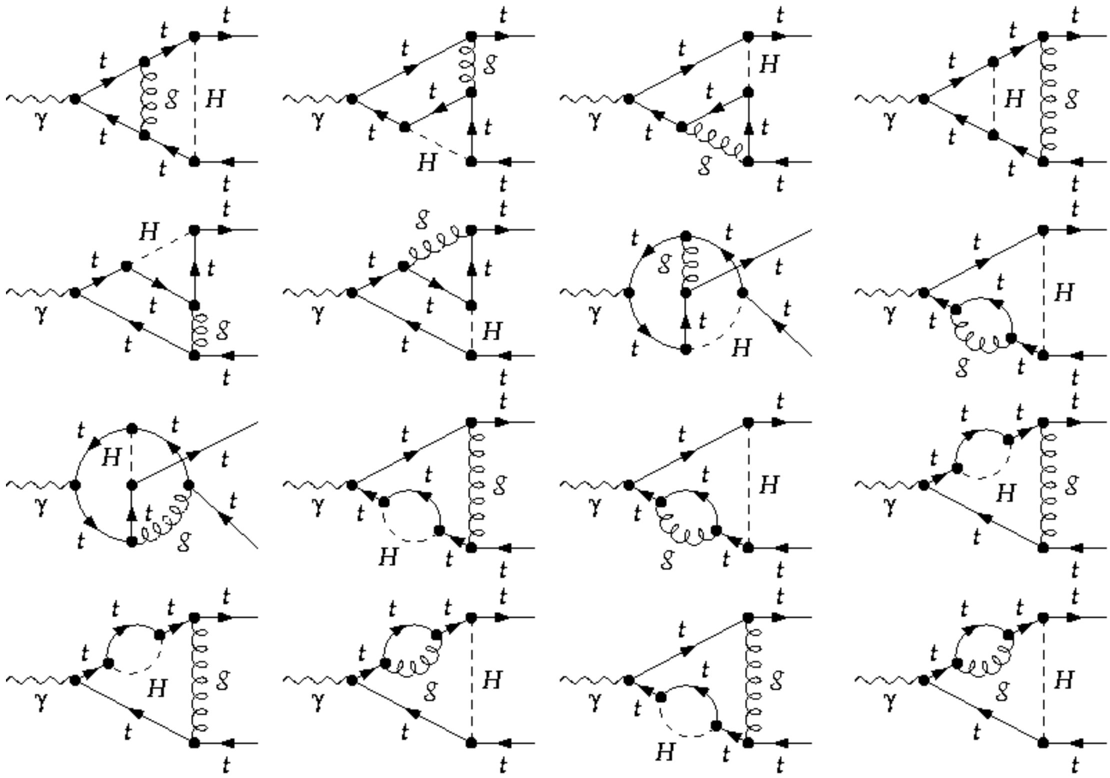

Figure 2: Two-loop Feynman diagrams contributing to $c_v^{H,\mathrm{mix}}$.

which makes the evaluation of the corresponding expansion terms quite tedious. This is particularly true for the two-loop order where due to the Coulomb divergence one will have a further factor m_t/M_h as compared to the one-loop term. Thus the expansion starts with a quartic top quark mass dependence. Furthermore, there are momentum regions which have $\sqrt{m_t/M_H}$ as expansion parameter.

On the other hand, as can be seen in Fig. 1, the result from this region is phenomenologically less important since for Higgs boson masses above 115 GeV there is perfect agreement between the exact result and the approximation one obtains for $m_t \approx M_h$ and $m_t \ll M_h$. Higgs boson masses below approximately 115 GeV are excluded by the direct search at the CERN Large Electron Positron Collider (LEP). For this reason we do not consider the limit $m_t \gg M_h$ at two-loop order.

Let us now turn to two loops. The Feynman diagrams are shown in Fig. 2. They are generated with `QGRAF` [20]. The application of `q2e` and `exp` [21,22] identifies the topology of the individual diagrams and adopts the notation in order to match one of the following functions

$$
\begin{aligned}
&J^{\pm}(n_1,n_2,n_3,n_4,n_5) = \\
&\quad \frac{e^{2\epsilon\gamma_E}}{(i\pi^{d/2})^2}\int \frac{\mathrm{d}^dk\mathrm{d}^dl}{(k^2+2kq)^{n_1}(l^2\pm 2lq)^{n_2}(k^2)^{n_3}((k-l)^2)^{n_4}(l^2-M^2)^{n_5}}\,, \\
&H^{\pm}_N(n_1,n_2,n_3,n_4,n_5) = \\
&\quad \frac{e^{2\epsilon\gamma_E}}{(i\pi^{d/2})^2}\int \frac{\mathrm{d}^dk\mathrm{d}^dl}{(k^2+2kq)^{n_1}(l^2\pm 2lq)^{n_2}(k^2)^{n_3}((k-l)^2-M^2)^{n_4}(l^2)^{n_5}}\,, \\
&Y^{\pm}_N(n_1,n_2,n_3,n_4,n_5) = \\
&\quad \frac{e^{2\epsilon\gamma_E}}{(i\pi^{d/2})^2}\int \frac{\mathrm{d}^dk\mathrm{d}^dl}{(k^2+2kq)^{n_1}(l^2\pm 2lq)^{n_2}((k-l)^2\mp 2q(k-l))^{n_3}(k^2)^{n_4}(l^2-M^2)^{n_5}}\,, \\
&Z^{+}_N(n_1,n_2,n_3,n_4,n_5) = \\
&\quad \frac{e^{2\epsilon\gamma_E}}{(i\pi^{d/2})^2}\int \frac{\mathrm{d}^dk\mathrm{d}^dl}{(k^2+2kq)^{n_1}(l^2+2lq)^{n_2}((k-l)^2-2q(k-l))^{n_3}(k^2-M^2)^{n_4}(l^2)^{n_5}}\,. \qquad (11)
\end{aligned}
$$

where $d=4-2\epsilon$ is the space-time dimension and the n_i are integer indices. The choice of the five-line integrals of Eq. (11) is possible due to the special kinematics we have at hand. Note that J^+, H^+ and Y^- correspond to self energies whereas J^-, H^-, Y^+ and Z^+ to vertex diagrams.

In a next step we use the program `AIR` [23] in order to reduce the integrals to about 30 master integrals. They range from very simple two-point expressions up to complicated two-scale integrals with five lines. At this point an asymptotic expansion in the various kinematical regions is performed. From the one-loop result (cf. Fig. 1) and from the considerations in the context of the on-shell wave function renormalization (see Ref. [13] and Appendix B) one can see that for the phenomenological interesting Higgs boson masses it is sufficient to have the expansion around $m_t \approx M_H$ and the one for $m_t \ll M_H$ at hand. Thus the master integrals are expanded in these two limits. In the case $m_t \approx M_H$ this reduces to a simple Taylor expansion whereas for $m_t \ll M_H$ the well-established hard-mass procedure [15] is applied. The latter is actually automated in the program `exp` [21,22]. Hence as an independent check we applied with the help of `exp` the hard-mass procedure to each diagram which immediately leads to simpler expressions and avoids the reduction to the master integrals. In this way the result for $m_t \ll M_h$ could be checked. We want to mention that the calculation has been performed for general QCD gauge parameter, ξ. The cancellation of ξ in the final result serves as a welcome check for our calculation.

As already mentioned in the Introduction, even after the proper combination of Z_2 and Γ_v is formed, as prescribed by Eq. (6), there remains an infra-red divergence which is plugged into $\tilde{Z}_v$. We subtract this divergence in the $\overline{\mathrm{MS}}$ scheme and introduce the anomalous dimension $\gamma_v = \frac{\mathrm{d}\ln\tilde{Z}_v}{\mathrm{d}\ln\mu}$ which is given by

$$
\gamma_v = -\frac{\alpha\alpha_s}{\pi^2 s_W^2}C_F\frac{\pi^2}{4}\frac{m_t^4}{M_W^2 M_h^2}\,. \qquad (12)
$$

In the regions $m_t \ll M_H$ and $m_t \approx M_H$ three, respectively, six expansion terms have been evaluated. Our results read

$$
\begin{aligned}
c_{v,0}^{H,\text{mix}} &= \frac{m_t^2}{M_W^2}\Bigg[\left(\frac{\pi^2}{8}\ln\frac{m_t^2}{\mu^2} - \frac{29}{216} - \frac{277\pi^2}{2304} - \frac{\pi^2\ln 2}{8} - \frac{21\zeta_3}{16} + \frac{139}{216}\ln y_H^2 \right.\\
&\quad \left. - \frac{103}{288}\ln^2 y_H^2\right) y_H^2 + \left(\frac{583}{576} - \frac{875\pi^2}{6912} + \frac{151}{192}\ln y_H^2 - \frac{17}{16}\ln^2 y_H^2\right) y_H^4 \\
&\quad + \left(\frac{1533691}{432000} - \frac{27103\pi^2}{138240} - \frac{66647}{43200}\ln y_H^2 - \frac{2251}{720}\ln^2 y_H^2\right) y_H^6 + \ldots\Bigg],\\
c_{v,1a}^{H,\text{mix}} &= \frac{m_t^2}{M_W^2}\Bigg[\frac{\pi^2}{8}\frac{1}{1-y_{H,1a}}\ln\frac{m_t^2}{\mu^2} - 5.760 - 5.533 y_{H,1a} \\
&\quad - 5.704 y_{H,1a}^2 - 5.888 y_{H,1a}^3 - 6.053 y_{H,1a}^4 - 6.200 y_{H,1a}^5 + \ldots\Bigg],\\
c_{v,1b}^{H,\text{mix}} &= \frac{m_t^2}{M_W^2}\Bigg[\frac{\pi^2}{8}(1-y_{H,1b})\ln\frac{m_t^2}{\mu^2} - 5.760 + 5.533 y_{H,1b} - 0.171 y_{H,1b}^2 \\
&\quad + 0.0124 y_{H,1b}^3 + 0.0304 y_{H,1b}^4 + 0.0296 y_{H,1b}^5 + \ldots\Bigg],
\end{aligned}
\qquad (13)
$$

where m_t is the on-shell mass and $\zeta_3 \approx 1.20206$ is Riemann's zeta-function. The $\ln(m_t^2/\mu^2)$ term reminds on the divergence which has been subtracted minimally. Since in the limit $m_t \ll M_H$ some coefficients of the ϵ-expansion of the master integrals could only be computed numerically the results for the finite parts of $c_{v,1a}^{H,\text{mix}}$ and $c_{v,1b}^{H,\text{mix}}$ are presented in numerical form. We also want to stress again that $c_{v,1a}^{H,\text{mix}}$ and $c_{v,1b}^{H,\text{mix}}$ contain the same information. However, expressed in terms of $y_{H,1b}$ the convergence properties are much better.

In Fig. 3 the results are shown where the same notation as for the one-loop result has been adopted and $\mu = m_t$ has been chosen. Next to the highest expansion terms we also include the lower-order terms as thin lines which nicely demonstrates the convergence properties in the individual regions. Comparing the two parameterizations of the expansion around $M_t = M_h$ one observes that the one in terms of $y_{H,1b}$ demonstrates a much better convergence behaviour: the thin dots in Fig. 3 are practically indistinguishable from the fat ones. This can also be seen in Eq. (13) where the coefficients become quite small starting from the third term which is not the case for $c_{v,1a}^{H,\text{mix}}$. Thus, the combination of $c_{v,1b}^{H,\text{mix}}$ and $c_{v,0}^{H,\text{mix}}$ provide a very good approximation to c_v^H for Higgs boson masses above $M_h = 115$ GeV.

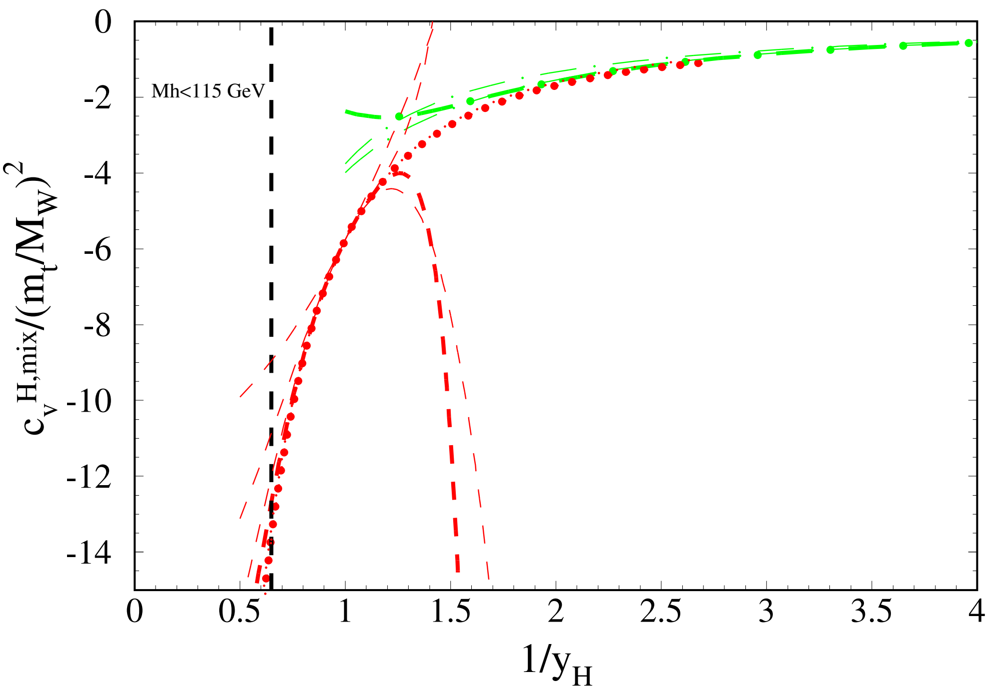

Figure 3: $c_v^{\rm mix}$ as a function of $1/y_H$. The approximations are shown as dotted, dashed and dash-dotted lines where for the expansion around $y_H \approx 1$ two different parameterizations have been chosen. Lower-order terms are plotted using thin lines. For the renormalization scale $\mu = m_t$ has been adopted.

4 Phenomenological application

Let us in a first step discuss the effect on the top quark mass. The connection between the position of the peak in the threshold cross section, $E_{\rm res}$, and the top quark mass is given by

$$E_{\rm res} \;=\; 2m_t + E_1^{\rm p.t.} + \delta^{\Gamma_t} E_{\rm res}\,, \tag{14}$$

where $E_1^{\rm p.t.}$ is the perturbative part of the ground state energy and $\delta^{\Gamma_t} E_{\rm res} = 100 \pm 10$ MeV [24] takes into account the effect of the finite width, the higher order resonances and the continuum. Non-perturbative effects are negligible for the top quark system. $E_1^{\rm p.t.}$ up to third order in QCD has been computed in Ref. [24]. The contribution from the Higgs boson is given in Eq. (2) where α_s has to be evaluated at the typical soft scale given by $\mu_s = C_F \alpha_s(\mu_s) m_t \approx 30$ GeV.

According to Eq. (14) a shift in $E_1^{\rm p.t.}$ can directly be translated into a shift in the top quark mass, δm_t. Choosing for the input values $m_t = 175$ GeV, $M_W = 80.41$ GeV, $s_W^2 = 0.23$, $\alpha = 1/127$ [25], $\alpha_s(M_Z) = 0.118$, $M_H = 120$ GeV and $\mu_s = 30$ GeV we observe for $\delta m_t \approx -E_1^H/2 \approx 26$ MeV. This reduces to 9(1) MeV for $M_H = 200(500)$ GeV. If $M_H = 120$ GeV is adopted and $\mu_s = 15(60)$ GeV is chosen one obtain $\delta m_t \approx 38(18)$ MeV. Thus, for light Higgs masses relatively large effects are observed whereas for larger M_H the numerical effect on m_t is small. Note that our findings are in agreement with the more qualitative analysis of Ref. [6].

As a second application it is interesting to consider the effect of the new corrections to the normalized cross section $R = \sigma(e^+e^- \to t\bar{t})/\sigma(e^+e^- \to \mu^+\mu^-)$ at the resonance energy which is dominated by the contribution from the would-be toponium ground-state. It is of the form

$$R_1 \;=\; R_1^{\rm LO} c_v^2(m_t) \frac{|\psi_1(0)|^2}{|\psi_1^C(0)|^2} + \ldots \tag{15}$$

with $R_1^{\rm LO} = 6\pi N_c Q_t^2 |\psi_1^C(0)|^2/\left(m_t^2\Gamma_t\right)$. The ellipses in Eq. (15) denote contributions from higher order operators. Note that the divergences in c_v and $\psi_1(0)$ cancel in the combination of Eq. (15). The most advanced evaluation of R_1 is provided in Ref. [4] where all logarithmically enhanced third-order corrections and the ones proportional to β_0^3 are included. Let us for completeness repeat the final numerical result which is given by

$$R_1 \;\approx\; R_1^{\rm LO}(1 - 0.244_{\rm NLO} + 0.449_{\rm NNLO} - 0.277_{\rm N^3LO'} + \delta_H^{(1)} + \delta_H^{(2)} \ldots)\,, \tag{16}$$

where $\mu_s = 30$ GeV has been chosen. The prime reminds that the N^{3}LO corrections are not complete and $\delta_H^{(1)}$ and $\delta_H^{(2)}$ parameterize the one- and two-loop corrections due to the Higgs boson considered in the present paper. Using $M_H = 120/200/500$ GeV and $\mu_s = 30$ GeV we obtain $\delta_H^{(1)} = 0.067/0.034/0.009$ and $\delta_H^{(2)} = 0.036/0.011/0.0002$. Thus, moderate effects are observed for Higgs boson masses below about 200 GeV. However, in contrast to the pure QCD effects of Eq. (16) the convergence seems to be much better as $\delta_H^{(2)}$ it is substantially smaller than $\delta_H^{(1)}$.

In principle it is possible to apply the formulae of this Section also to the bottom system. However, due to the suppression factor m_b^2/M_H^2 the numerical effect is very small for Higgs boson masses above 100 GeV.

5 Conclusions

In this paper we take an important step towards the evaluation of the mixed QCD/electroweak corrections to the threshold production of top quark pairs, namely, the complete Higgs boson mass dependence is computed. In particular, the two-loop corrections to the matching coefficients are evaluated and the corresponding operator is introduced in the effective theory. Moderate numerical effects on the top quark mass and the peak cross section are observed for Higgs boson masses below 200 GeV. Considering the anticipated precision of an ILC it is certainly necessary to take into account these corrections.

Acknowledgements

We would like to thanks J.H. Kühn, A.A. Penin, V.A. Smirnov and O.V. Tarasov for useful discussions and A.A. Penin for carefully reading the manuscript. This work was supported by the "Impuls- und Vernetzungsfonds" of the Helmholtz Association, contract number VH-NG-008 and the SFB/TR 9.

A Matching coefficients for the Z boson exchange diagrams

In the following we present the results for the matching coefficients induced by vertex corrections involving the Z boson and the corresponding Goldstone boson, respectively. The calculation is similar to the diagrams involving a Higgs boson which is presented in the main part of the paper. Note that there are also box diagrams involving the Z boson which are not considered here. The one-loop result is given by [16]

$$\begin{aligned} c_v^{Z,\mathrm{ew}} &= a_t^2 s_W^2 \left[\frac{5y_Z^2-2}{12y_Z^2} - \frac{3y_Z^4-4y_Z^2+1}{12y_Z^4}\ln y_Z^2 + \frac{(y_Z^2-1)^2}{6y_Z^2}\Psi(y_Z)\right] \\ &\quad + v_t^2 s_W^2 \left[-\frac{3y_Z^2+2}{12y_Z^2} - \frac{1}{12y_Z^4}\ln y_Z^2 + \left(\frac{7}{48}+\frac{1}{6y_Z^2}+\frac{y_Z^2}{4}-\frac{3}{16(4y_Z^2-1)}\right)\Psi(y_Z)\right], \end{aligned} \tag{17}$$

with $y_Z = m_t/M_z$, $a_t = 1/(2s_W c_W)$, $v_t = (1/2 - 4s_W^2/3)/(s_W c_W)$ and $c_W = \sqrt{1-s_W^2} = M_W/M_Z$. The function $\Psi(x)$ can be found in Eq. (9). It is straightforward to obtain the expansion in the various kinematical regions. Thus we refrain from listing them explicitly. In Fig. 4(a) the exact result is plotted together with the expansions where in each region the same depth is chosen as in Eq. (10). The vertical dashed line marks the phenomenological result for y_Z which is nicely approximated both from the $m_t \gg M_Z$ and the $m_t \approx M_Z$ region. However, it should be noted that both parameterizations for the $m_t = M_h$ expansion become instable below $1/y_Z \approx 0.6$.

At two-loop order we consider the diagrams of Fig. 2 where the Higgs boson is replaced by the Z boson. The reduction of the occuring integrals is in close analogy and in fact the same set of master integrals is necessary. Although the region $m_t \ll M_Z$ is phenomenologically not relevant we nevertheless present the results since it constitutes an important cross checks for the other kinematical limits. Furthermore, it is possible to obtain from this limit the result for the case of the bottom quark. We adopt the notation from Eq. (7) and denote the contribution from the Z boson to c_v^{mix} by $c_v^{Z,\mathrm{mix}}$. The additional subscript "0", "1a" or "1b" reminds on the kinematical region considered.

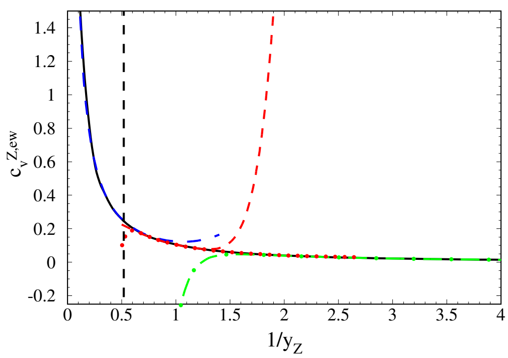

(a)

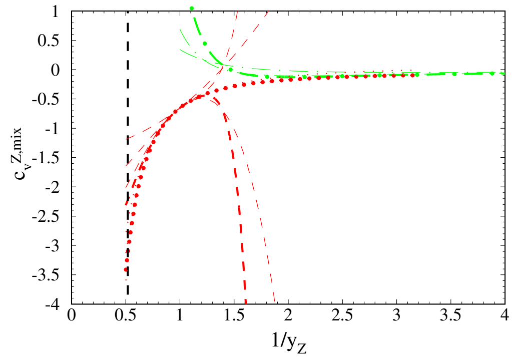

(b)

Figure 4: (a) $c_v^{Z,\mathrm{ew}}$ and (b) $c_v^{Z,\mathrm{mix}}$ as a function of $1/y_Z$. The same notation as in Figs. 1 and 3 is adopted. The vertical line indicates the physical value of $1/y_Z = M_Z/m_t$.

Our results read

$$
\begin{aligned}
c_{v,0}^{Z,\mathrm{mix}} \quad = \quad & \left(v_t^2 + a_t^2\right) s_W^2 \frac{\pi^2}{8} \ln \frac{m_t^2}{\mu^2} \\
& + v_t^2 s_W^2 \left[\left(-\frac{587}{432} + \frac{131\pi^2}{576} - \frac{\pi^2 \ln 2}{8} - \frac{21}{16}\zeta_3 + \frac{28}{27} \ln y_Z^2 - \frac{11}{72} \ln^2 y_Z^2 \right) y_Z^2 \right. \\
& + \left(-\frac{403}{64} + \frac{205\pi^2}{576} + \frac{2299}{864} \ln y_Z^2 - \frac{5}{18} \ln^2 y_Z^2 \right) y_Z^4 \\
& \left. + \left(-\frac{21091951}{864000} + \frac{3951\pi^2}{2560} + \frac{28301}{7200} \ln y_Z^2 + \frac{469}{160} \ln^2 y_Z^2 \right) y_Z^6 + \dots \right] \\
& + a_t^2 s_W^2 \left[\left(-\frac{281}{432} + \frac{85\pi^2}{192} - \frac{\pi^2 \ln 2}{8} - \frac{21}{16}\zeta_3 + \frac{29}{54} \ln y_Z^2 - \frac{11}{72} \ln^2 y_Z^2 \right) y_Z^2 \right. \\
& + \left(\frac{709}{576} + \frac{11\pi^2}{432} + \frac{521}{288} \ln y_Z^2 - \frac{79}{72} \ln^2 y_Z^2 \right) y_Z^4 \\
& \left. + \left(\frac{260687}{32000} - \frac{16013\pi^2}{69120} + \frac{32453}{21600} \ln y_Z^2 - \frac{5479}{1440} \ln^2 y_Z^2 \right) y_Z^6 + \dots \right],
\end{aligned}
$$

$$
\begin{aligned}
c_{v,1a}^{Z,\mathrm{mix}} &= \left(v_t^2+a_t^2\right)s_W^2\frac{\pi^2}{8}\ln\frac{m_t^2}{\mu^2}\frac{1}{1-y_{Z,1a}}\\
&\quad+v_t^2 s_W^2\Bigg[-4.564-4.699y_{Z,1a}-5.009y_{Z,1a}^2-5.277y_{Z,1a}^3-5.502y_{Z,1a}^4\\
&\quad-5.693y_{Z,1a}^5+\ldots\Bigg]+a_t^2 s_W^2\Bigg[-1.324-1.504y_{Z,1a}-1.740y_{Z,1a}^2\\
&\quad-1.930y_{Z,1a}^3-2.083y_{Z,1a}^4-2.212y_{Z,1a}^5+\ldots\Bigg],
\end{aligned}
$$

$$
\begin{aligned}
c_{v,1b}^{Z,\mathrm{mix}} &= \left(v_t^2+a_t^2\right)s_W^2\frac{\pi^2}{8}\ln\frac{m_t^2}{\mu^2}\left(1-y_{Z,1b}\right)+v_t^2 s_W^2\Bigg[-4.564+4.699y_{Z,1b}\\
&\quad-0.311y_{Z,1b}^2-0.043y_{Z,1b}^3+0.001y_{Z,1b}^4+0.011y_{Z,1b}^5+\ldots\Bigg]\\
&\quad+a_t^2 s_W^2\Bigg[-1.324+1.504y_{Z,1b}-0.236y_{Z,1b}^2-0.047y_{Z,1b}^3-0.011y_{Z,1b}^4\\
&\quad-0.001y_{Z,1b}^5+\ldots\Bigg],
\end{aligned}
\tag{18}
$$

where the divergence has been subtracted in a minimal way and $y_Z = m_t/M_Z$, $y_{Z,1a} = (1-1/y_Z^2)$ and $y_{Z,1b} = (1-y_Z^2)$. In Fig. 4(b) the results of Eq. (18) are shown as a function in $1/y_Z$. Similarly to the two-loop case one observes a rapid convergence for $c_{v,1b}^{Z,\mathrm{mix}}$ whereas the magnitude of the coefficients of the higher order terms in $c_{v,1a}^{Z,\mathrm{mix}}$ even increase. This gives us quite some confidence that $c_{v,1b}^{Z,\mathrm{mix}}$ evaluated at the physical scale provides a very good approximation to the unknown exact result. Using $1/y_Z = 91.19/175 \approx 0.52$ we get

$$
c_v^{Z,\mathrm{mix}}\Bigg|_{\mu^2=m_t^2} \approx -3.1\pm 0.3\,,
\tag{19}
$$

where we assign a generous uncertainty of 10% which results from the comparison of lower-order approximations. The accuracy of the result for $c_v^{Z,\mathrm{mix}}$ as given in Eq. (19) is more than sufficient as far as the forseen precision of the measurement of the threshold top quark production is concerned.

B Addendum to Ref. [13]

In this Appendix we want to provide an update of the results of Ref. [13]. In Fig. 4 of that reference the Higgs boson mass dependence of the on-shell wave function renormalization

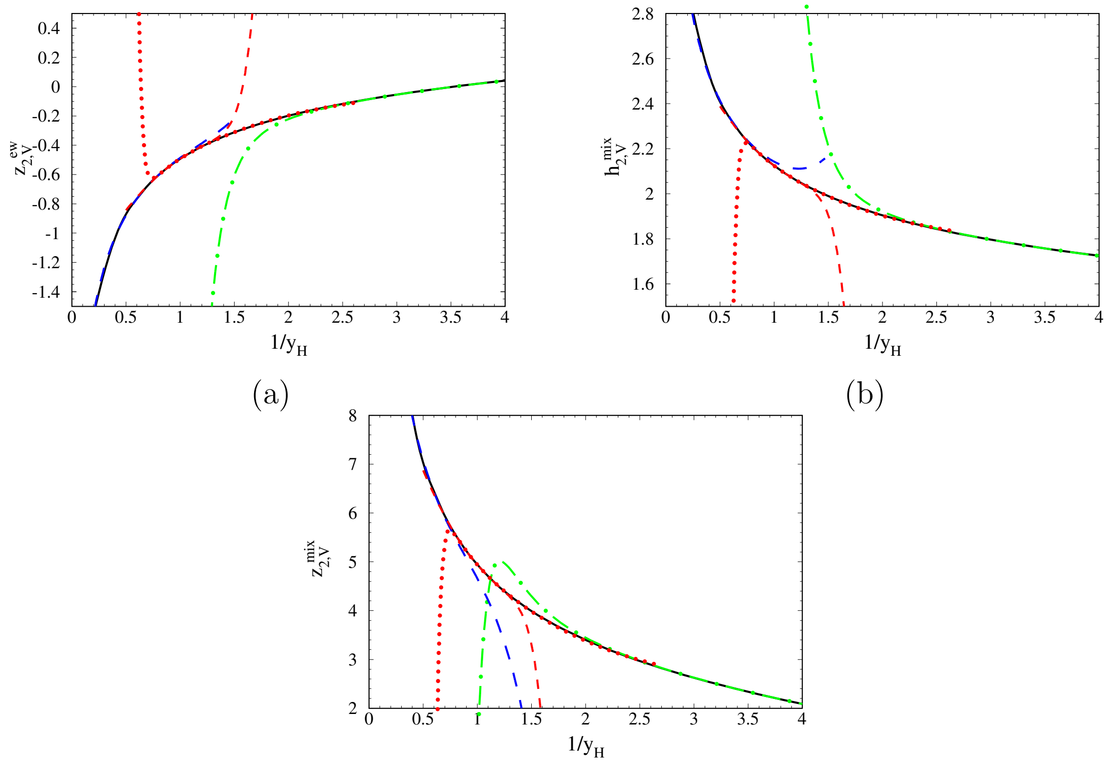

(c)

Figure 5: (a) One-loop, (b) $1/\epsilon$ pole and (c) constant part of the two-loop corrections to $Z_2^{V,\mathrm{OS}}$ as a function of $1/y_H = M_H/m_t$. The solid (black) line represents the exact result. The approximations in the three regions are shown as dotted, dashed and dash-dotted lines where for the expansion around $y_H \approx 1$ two different parameterizations (short dashes and dots) have been chosen.

constant to one- and two-loop order has been plotted as a function of $1/y_H = M_H/m_t$. Next to the exact results also the ones for $m_t \ll M_H$, $m_t \approx M_H$ and $m_t \gg M_H$ have been shown and good agreement over almost the whole range in y_H has been found. However, there was a small gap around $1/y_H \approx 2$ which was not covered very well. This deficit is removed in Fig. 5 where the result obtained in the limit $m_t \approx M_H$ is plotted both in terms of $y_{H,1a} = (1 - 1/y_H^2)$ (dashed) and $y_{H,1b} = (1 - y_H^2)$ (dotted). One can see that the former is valid down to quite small values of $1/y_H$ whereas the validity of the latter expansion reaches up to larger values of $1/y_H$ leading to a significant overlap with the expansions for large and small values of y_H. Thus, in the whole y_H range the simple expansions approximate the exact result to a very high precision.

Let us also mention that there is a misprint in the definition of v_t in Ref. [13] after Eq. (17): it is too small by a factor two. Furthermore, the analytic expression for Y^ϵ in Eq. (22) has to be multiplied by (-1) and in Eq. (27) a factor $1/s_W^2$ is missing in the terms containing α_s/π.

References

[1] see, e.g., `http://linearcollider.org/`

[2] M. Martinez and R. Miquel, Eur. Phys. J. C **27** (2003) 49.

[3] A. H. Hoang *et al.*, Eur. Phys. J. directC **2** (2000) 1 [arXiv:hep-ph/0001286].

[4] A. A. Penin, V. A. Smirnov and M. Steinhauser, Nucl. Phys. B **716** (2005) 303 [arXiv:hep-ph/0501042].

[5] M. Beneke, Y. Kiyo and K. Schuller, Nucl. Phys. B **714** (2005) 67 [arXiv:hep-ph/0501289].

[6] M. J. Strassler and M. E. Peskin, Phys. Rev. D **43** (1991) 1500.

[7] A. H. Hoang and C. J. Reisser, Phys. Rev. D **71** (2005) 074022 [arXiv:hep-ph/0412258].

[8] A. H. Hoang and C. J. Reisser, arXiv:hep-ph/0604104.

[9] W. E. Caswell and G. P. Lepage, Phys. Lett. B **167** (1986) 437.

[10] G. T. Bodwin, E. Braaten and G. P. Lepage, Phys. Rev. D **51** (1995) 1125 [Erratum-ibid. D **55** (1997) 5853] [arXiv:hep-ph/9407339].

[11] B. A. Kniehl, A. A. Penin, V. A. Smirnov and M. Steinhauser, Nucl. Phys. B **635** (2002) 357 [arXiv:hep-ph/0203166].

[12] B. A. Kniehl, A. A. Penin, M. Steinhauser and V. A. Smirnov, Phys. Rev. Lett. **90** (2003) 212001 [arXiv:hep-ph/0210161].

[13] D. Eiras and M. Steinhauser, JHEP **0602** (2006) 010 [arXiv:hep-ph/0512099].

[14] M. Beneke and V. A. Smirnov, Nucl. Phys. B **522** (1998) 321 [arXiv:hep-ph/9711391].

[15] V.A. Smirnov, Applied Asymptotic Expansions in Momenta and Masses, Springer-Verlag, Berlin-Heidelberg, 2001.

[16] R. J. Guth and J. H. Kühn, Nucl. Phys. B **368** (1992) 38.

[17] A. Czarnecki and K. Melnikov, Phys. Rev. Lett. **80** (1998) 2531 [arXiv:hep-ph/9712222].

[18] M. Beneke, A. Signer and V. A. Smirnov, Phys. Rev. Lett. **80** (1998) 2535 [arXiv:hep-ph/9712302].

[19] B. A. Kniehl, A. Onishchenko, J. H. Piclum and M. Steinhauser, arXiv:hep-ph/0604072, Phys. Lett. B (in print).

[20] P. Nogueira, J. Comput. Phys. **105** (1993) 279.

[21] R. Harlander, T. Seidensticker and M. Steinhauser, Phys. Lett. B **426** (1998) 125 [hep-ph/9712228].

[22] T. Seidensticker, hep-ph/9905298.

[23] C. Anastasiou and A. Lazopoulos, JHEP **0407** (2004) 046 [arXiv:hep-ph/0404258].

[24] A. A. Penin and M. Steinhauser, Phys. Lett. B **538** (2002) 335 [arXiv:hep-ph/0204290].

[25] F. Jegerlehner, arXiv:hep-ph/0105283.